Frequency-Dependent Kinetics and Prevalence of Kiss-and-Run and Reuse at Hippocampal Synapses Studied with Novel Quenching Methods

Nobutoshi C. Harata,[1] Sukwoo Choi,[2] Jason L. Pyle,[1] Alexander M. Aravanis,[1] and Richard W. Tsien[1,*]
[1] Department of Molecular and Cellular Physiology
Stanford University School of Medicine
Stanford, California 94305
[2] Seoul National University
School of Biological Sciences
Kwanak Gu
Sillim 9 Dong San 56-11
Seoul 151-742
South Korea

Summary

The kinetics of exo-endocytotic recycling could restrict information transfer at central synapses if neurotransmission were entirely reliant on classical full-collapse fusion. Nonclassical fusion retrieval by kiss-and-run would be kinetically advantageous but remains controversial. We used a hydrophilic quencher, bromophenol blue (BPB), to help detect nonclassical events. Upon stimulation, extracellular BPB entered synaptic vesicles and quenched FM1-43 fluorescence, indicating retention of FM dye beyond first fusion. BPB also quenched fluorescence of VAMP (synaptobrevin-2)-EGFP, thus indicating the timing of first fusion of vesicles in the total recycling pool. Comparison with FM dye destaining revealed that kiss-and-run strongly prevailed over full-collapse fusion at low frequency, giving way to a near-even balance at high frequency. Quickening of kiss-and-run vesicle reuse was also observed at higher frequency in the average single vesicle fluorescence response. Kiss-and-run and reuse could enable hippocampal nerve terminals to conserve scarce vesicular resources when responding to widely varying input patterns.

Introduction

Full-collapse fusion, first described at the neuromuscular junction in elegant studies of Heuser, Reese, and others (Heuser, 1989; Heuser and Reese, 1973; Koenig and Ikeda, 1996; Miller and Heuser, 1984), has also been found in CNS nerve terminals (Aravanis et al., 2003a; Gandhi and Stevens, 2003; Klyachko and Jackson, 2002; Li and Murthy, 2001; Richards et al., 2005; Sankaranarayanan and Ryan, 2000, 2001; Zenisek et al., 2002). In this classical mode, vesicle fusion establishes complete aqueous continuity between vesicle lumen and external medium, and full lipid continuity between vesicle membrane and plasma membrane. There is mounting evidence for an additional, nonclassical mode of fusion, generically termed "kiss-and-run" (Valtorta et al., 2001), in which vesicles fuse transiently with the plasma membrane without complete loss of identity (Ceccarelli et al., 1973). Kiss-and-run fusion has been contrasted with

full-collapse fusion on several grounds, including vesicle location after fusion (Sudhof, 2004), lack of lipid or protein continuity between vesicle and cell membrane (An and Zenisek, 2004), or involvement of specific proteins in vesicle retrieval (Ryan, 2003; Stevens and Williams, 2000). Other labels for nonclassical phenomena include "cavicapture," "rapid endocytosis," "kiss-and-stay," and "flicker." The multiplicity of terms reflects growing consensus that nonclassical fusion exists but also lack of agreement on its critical features (An and Zenisek, 2004; Palfrey and Artalejo, 1998; Rizzoli and Betz, 2005; Royle and Lagnado, 2003; Ryan, 2003; Sudhof, 2004; Wu, 2004).

For the small nerve terminals predominant in brain, defining key features of fusion modes is particularly important because of their potential impact on synaptic information transfer. After classical full collapse, vesicle retrieval and repriming require several tens of seconds (Liu and Tsien, 1995; Ryan et al., 1993), and would thus impose a temporal bottleneck in presynapses containing only ∼30 recycling vesicles (Harata et al., 2001). Kiss-and-run offers a way out of this kinetic dilemma but is incompletely defined in the very terminals where it would do the most good. Some key questions are as follows.

Does kiss-and-run exist in small CNS boutons, and does it extend to the total recycling pool (TRP)? In support of kiss-and-run at hippocampal nerve terminals, synaptic vesicles preloaded with FM1-43 (Cochilla et al., 1999) partially retained the lipophilic dye even after fusion, reflecting a transient connection between vesicle interior and external milieu (Klingauf et al., 1998; Pyle et al., 2000; Sara et al., 2002). The retention was seen most clearly in destaining of single synaptic vesicles (Aravanis et al., 2003a, 2003b; Richards et al., 2005). Experiments with an intravesicular pH indicator protein, synaptopHluorin, pinned down the delay between vesicle fusion and retrieval to <0.9 s (Gandhi and Stevens, 2003). Nonclassical fusion has received support in other synaptic systems as well (Staal et al., 2004; Verstreken et al., 2002) (but see Dickman et al., 2005), but no consensus has been reached about its defining features. Is kiss-and-run an exclusive property of vesicles residing for some time in the readily releasable pool (RRP) (Pyle et al., 2000; Sara et al., 2002), or does it extend to the TRP? Because of confusion about the defining features of kiss-and-run, its very existence has been disputed (Fernandez-Alfonso and Ryan, 2004).

Can recycled vesicles be immediately reused, and what are the kinetics of first fusion and reuse? Reuse of vesicles that have fused by kiss-and-run would be advantageous for increasing the synaptic throughput allowed by a small number of recycling vesicles (Pyle et al., 2000; Sara et al., 2002). Evidence indicates that vesicles can be retrieved with intact exocytotic machinery, undergo rapid reloading with neurotransmitter, and support multiple rounds of neurotransmitter release. To delineate reuse clearly, one needs to distinguish the kinetics of first fusion (first exocytosis of naive vesicles after a rest period without stimulation) and subsequent reuse. Such distinctions have not been possible with

*Correspondence: rwtsien@stanford.edu
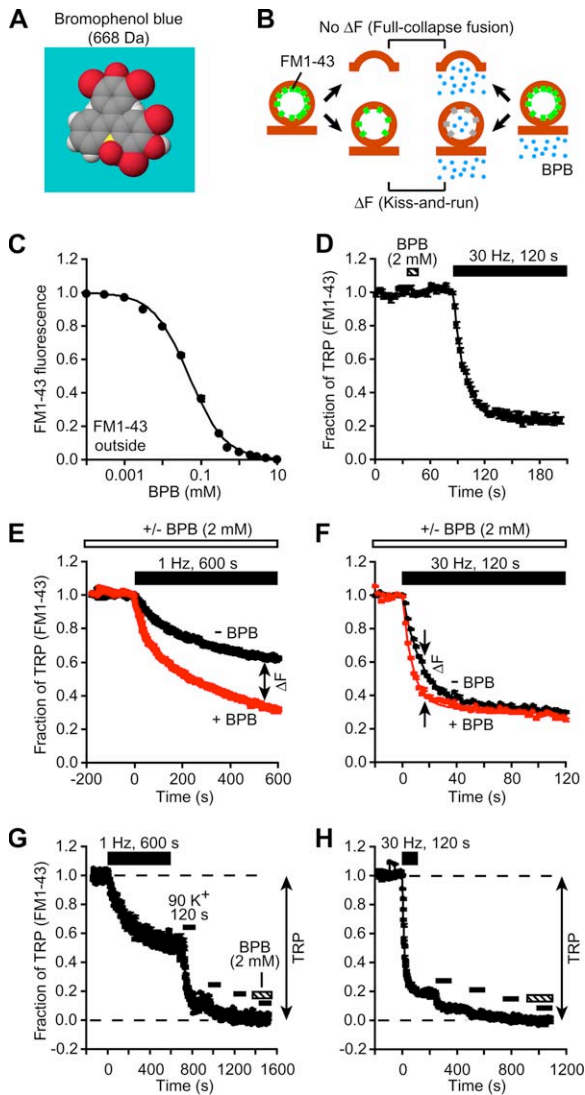
Figure 1. FM1-43 Was Retained in Synaptic Vesicles Even after First Fusion

(A) Structure of a quencher, BPB. Dark gray, carbon; light gray, hydrogen; large red, bromine; small red, oxygen; yellow, sulfur. (B) Diagram contrasting different fusion modes and loss of FM1-43 fluorescence with extracellular BPB (blue dots). With full-collapse fusion (top), BPB induces no fluorescence difference signal (no ΔF), but with kiss-and-run (bottom), BPB induces significant ΔF by quenching FM1-43 lingering in synaptic vesicles (gray). (C and D) Properties of FM1-43 quenching by BPB. (C) Concentration-quenching curve obtained on the plasma membrane. [FM1-43] = 7.5 μM. IC_{50} = 0.05 mM; n_H = 0.92. n = 70 regions of interest (three coverslips). (D) BPB application to boutons at rest did not affect FM1-43 loaded into synaptic vesicles or subsequent destaining. n = 103 boutons (two coverslips). (E and F) FM1-43 was retained in vesicles regardless of whether boutons were destained at 1 Hz (E) or 30 Hz (F). FM1-43 destaining was faster in 2 mM BPB (red symbols) than in its absence (black symbols) (ΔF), reflecting the rapid closure of fusion pores and the presence of kiss-and-run. n = 146–253 boutons (three to four coverslips). (G and H) Definition of total recycling pool (TRP). After staining with FM1-43, boutons were destained with field stimulation at various frequencies, followed by three rounds of 90 K^+ stimulation. A final K^+ stimulation in the presence of 2 mM BPB did not lead to any detectable fluorescence loss. Total fluorescence loss was used to define TRP. n = 50 (G) and n = 45 boutons (H) from representative coverslips. In (C)–(H), data points represent mean ± SEM. Many of the SEM bars were smaller than the symbols.

recordings of presynaptic capacitance, postsynaptic currents, or amperometrically monitored transmitter release, which cannot distinguish between first-time fusion and events arising from recycled, reloaded vesicles. Imaging of single FM1-43-loaded vesicles shows FM dye release in a series of discrete down steps (Aravanis et al., 2003b), but this only demonstrates reuse for RRP vesicles, not the whole TRP.

Does the balance between full-collapse and nonclassical fusion vary with stimulation frequency? The reported incidence of kiss-and-run ranges greatly, from as low as ~5% during spontaneous release in neuroendocrine cells (Ales et al., 1999; Klyachko and Jackson, 2002), up to 25% (Gandhi and Stevens, 2003) or 85% (Aravanis et al., 2003a) in low-frequency release evoked from hippocampal neurons. Little is known about the prevalence of kiss-and-run over the wide range of spike frequency that hippocampal neurons experience in vivo, typically averaging ~1 Hz but increasing to 5–20 Hz for sustained periods and >50 Hz in brief bursts.

None of these questions can be readily answered with existing methodologies. Accordingly, we have developed two new assays, both involving the suppression of intravesicular fluorescence by entry of a hydrophilic quencher, and applied them to delineate the frequency-dependent properties of kiss-and-run and reuse. The quencher, bromophenol blue (BPB), enters synaptic vesicles during fusion and quenches FM1-43 or EGFP tagged to the lumenal side of the vesicle. Using these methods, we provide definitive evidence that FM1-43 was partially retained in vesicles during first fusion but later released during extended stimulation, and that the prevalence of kiss-and-run was strongly frequency dependent, increasing to 80% at low frequency. We describe the kinetics of first fusion and the rate of reuse, key kinetic parameters that govern vesicle performance in support of synaptic information transfer.

Results

BPB Quenching Verifies FM1-43 Trapping in Synaptic Vesicles

We took a new approach to test whether FM1-43 is partially retained in synaptic vesicles even after exocytosis, using BPB to quench the green emission of trapped FM dye. BPB shares some features with fast neurotransmitters (Figure 1A): it is negatively charged between pH 5.6 and 7.4, and its longest dimension is ~1.5 nm, comparable to glutamate (~1.0 nm). Our use of BPB was motivated as follows: if all exocytosis occurs by classical full-collapse fusion and/or lipid continuity, FM dye in vesicles would rapidly leave the hydrophobic environment in the region of interest, causing almost immediate fluorescence loss following exocytosis (Figure 1B). Thus, little or no additional effect of fluorescence quenching (no ΔF) would be expected upon entry of BPB into the vesicle lumen. But for exocytotic events followed by rapid vesicular retrieval, FM dye would be retained in the vesicle long after first fusion; BPB entry would then quench the remaining intravesicular fluorescence, thus producing a difference signal (ΔF).

We first assessed how efficiently BPB quenches FM1-43. In the maintained presence of FM1-43, we applied various concentrations of BPB to cultured

hippocampal neurons and measured changes in fluorescence intensity. This measurement largely registered membrane fluorescence rather than solution fluorescence because the quantum yield of FM1-43 is much larger in a hydrophobic environment (Cochilla et al., 1999). BPB quenched the plasma membrane fluorescence in a concentration-dependent manner (Figure 1C). However, BPB did not quench FM1-43 in vesicles at rest (Figure 1D), verifying that BPB cannot easily pass through membranes, consistent with its hydrophilic nature. It also indicated that the quenching requires close proximity to the fluorophore and cannot occur when the quencher and fluorescent indicator are separated by cell and vesicle membranes (for discussion of possible quenching mechanisms, see the Supplemental Experimental Procedures in the Supplemental Data available with this article online).

After conventional FM dye staining, we monitored the activity-dependent decay of FM1-43 fluorescence upon stimulation. At either 1 Hz or 30 Hz (Figures 1E and 1F), the presence of 2 mM BPB markedly speeded the fluorescence loss. The fluorescence difference (ΔF) was highly significant, developing prominently with 360 stimuli at 1 Hz, and developing but then largely disappearing after 1800 stimuli at 30 Hz. A similar acceleration of fluorescence loss by BPB was observed when the FM1-43 concentration for staining was reduced from 7.5 to 2.5 μM, or when the number of stimuli for FM1-43 staining was increased from 1200 to 3600 (data not shown), thus showing the robustness of the assay system. Changes in BPB concentration ([BPB]) led to different amounts of ΔF (Figure S1A), corresponding to different efficiencies of quenching (Figure 1C; see Figure 5 for rationale). A similar ΔF was observed when the temperature was raised from ~23°C to ~33°C (Figure S1B). In all of these tests, fluorescence signals were carefully referred to the TRP for each bouton under study, taking account of further fluorescence loss during three rounds of destaining with 90 mM K$^+$ solution following the field stimulation (Figures 1G and 1H). The third round produced little or no drop in fluorescence, indicating that hardly any releasable FM dye remained. As an additional check that a reliable baseline had been reached, exposure to K$^+$-rich solution in the presence of BPB produced no further fluorescence loss. To test the effects of BPB application on vesicle recycling, synapses were stained with the red dye FM4-64 and destained by high-K$^+$ depolarization. FM4-64 destaining kinetics were the same in the absence or presence of 2 mM BPB (Figure S3A), indicating that BPB did not compromise vesicle recycling.

Contrary to predictions of classical full-collapse fusion alone, these results established that vesicles can retain FM dye for extended periods after they first fuse. There must be a mechanism that prevents FM1-43 from escaping from vesicles during a single fusion event, for example, the reclosing of the fusion pore. In addition, BPB molecules must be able to enter the vesicle lumen during its transient connection with the external solution.

BPB Quenching of VAMP-EGFP Tracks First-Time Exocytosis
The use of a diffusible quencher offers a new way to gain quantitative information about fusion events. In the ideal

case, the target fluorophore would be persistently associated with the vesicle interior, unlike FM dye, while only the vesicular concentration of quencher would vary (Figure 2A). EGFP is well suited for this purpose: while negligibly quenched by H$^+$ at pH 7, EGFP displays spectral properties that allow efficient quenching by BPB and can come fused with the lumenal domain of the vesicular protein VAMP-2 (synaptobrevin-2). When expressed by transfection of cultured hippocampal neurons, VAMP-EGFP appeared in puncta, strongly correlated in position and intensity with puncta of FM4-64 (Figure S2A), confirming its primary localization in actively recycling presynaptic boutons. Although EGFP fluorescence is pH sensitive, potential complications of pH changes in vesicles were avoided by eliminating their pH gradient with a H$^+$ pump inhibitor, bafilomycin A1 (Figure S2B).

The basic properties of BPB-induced quenching are illustrated in Figures 2B–2G. In the absence of BPB, field stimulation of exo-endocytosis produced no change in EGFP fluorescence (Figure 2C), verifying that bafilomycin treatment had eliminated any confounding pH changes. Exposing resting terminals to BPB quenched part of the basal fluorescence signal (Figures 2B and 2C), that arose from VAMP-EGFP on the plasma membrane at rest (Li and Murthy, 2001; Sankaranarayanan et al., 2000), most likely due to mistargeting. Vesicular fluorescence was evident in the more circular and discrete fluorescent spots that remained; subsequent stimulation in the presence of BPB strongly reduced the fluorescence (Figures 2B and 2C). The BPB quenching induced by depolarizing stimuli was abolished in the absence of extracellular Ca^{2+} (data not shown). Thus, the stimulus-induced quenching required both BPB and extracellular Ca^{2+}, as expected if the quenching depended on Ca^{2+}-dependent fusion and subsequent entry of BPB into the vesicle lumen. After BPB had entered vesicles, washout of external BPB allowed recovery of surface VAMP-EGFP fluorescence (Figure 2D, broken line). A second round of stimulation then induced a further rise in fluorescence (Figure 2D), indicating that BPB that had been trapped within vesicles was able to depart from them during further vesicle turnover. These results showed that entry and exit of BPB were activity dependent, and that quenching of intraluminal EGFP was reversible.

The concentration dependence of BPB quenching was assessed by focusing on VAMP-EGFP expressed on the external surface of neurons (Figure 2E). Quenching was rapid, reversible, and near maximal at 2–3 mM. Indeed, the quenching produced by 2 mM BPB was equal to that rendered by acidification to pH 4 (Figure S2C), a treatment known to abolish EGFP fluorescence (Sankaranarayanan et al., 2000). As a control, we applied BPB to HEK293 cells expressing EGFP tethered on the cytoplasmic side of the plasma membrane, by fusion with the N terminus of α_{1C} L-type Ca^{2+} channel subunits. Thus segregated from the extracellular solution, EGFP was not quenched by external BPB (Figure 2E), consistent with our findings with FM1-43 compartmentalized in vesicles (Figure 1D). Finally, BPB quenching of surface VAMP-EGFP (Figure 2D; Figure S2C) and of surface FM1-43 (data not shown) were reversed completely and rapidly (<3 s) following BPB washout. Thus, proteins and lipids on the surface membrane, and by
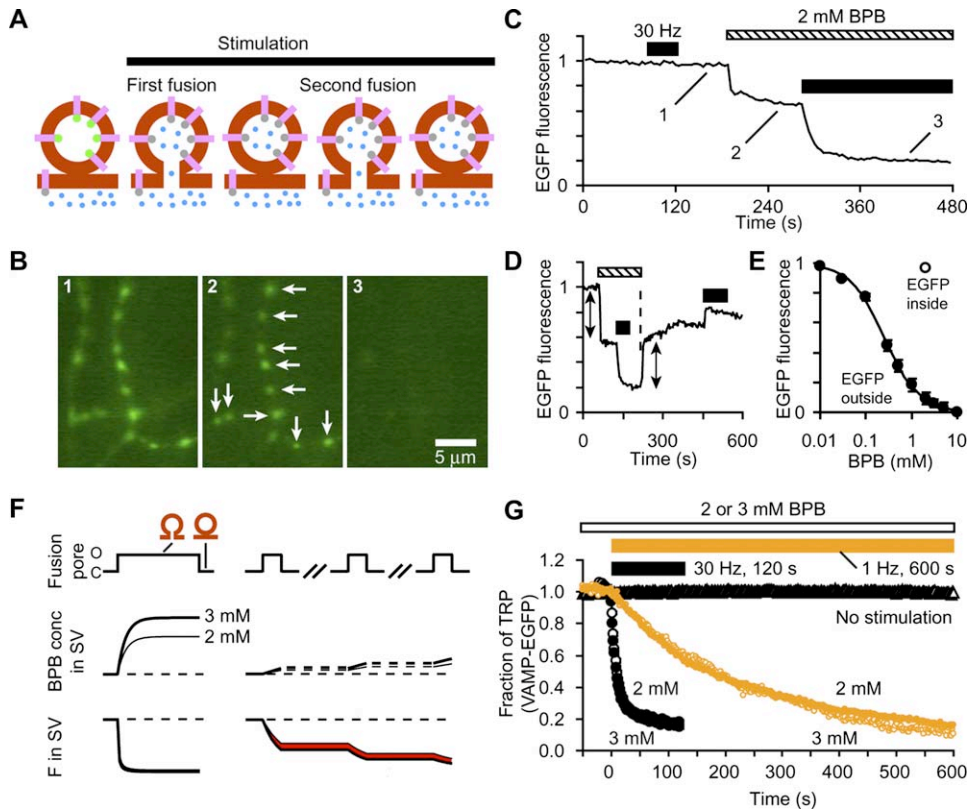
Figure 2. Quenching of Vesicular VAMP-EGFP by BPB Reports First Fusion Events

(A) Schematic illustrating how BPB accesses EGFP in neurons expressing VAMP-EGFP. Bath-applied BPB (blue dots) will enter synaptic vesicles during the first exocytotic event and quench EGFP fluorescence (changing from green to gray) on the lumenal side of VAMP (magenta). EGFP will remain quenched in the continued presence of BPB even if the same vesicle undergoes repeated fusion. (B and C) Vesicular EGFP fluorescence was quenched only when exo-endocytosis was induced in the presence of BPB. Fluorescence image shows representative boutons before BPB application (B1; point C1). Field stimulation (filled bar) alone failed to change fluorescence, confirming the abolition of pH gradient. Boutons were then exposed to BPB to eliminate surface VAMP-EGFP fluorescence (B2; point C2). In B2, arrows denote examples of fluorescence remaining in vesicles that was strongly reduced upon subsequent field stimulation (B3; point C3). (C) Trace showing average data from 59 boutons in a representative experiment. (D) Quenching of surface and vesicular VAMP-EGFP was reversible. After quenching of vesicular VAMP-EGFP, as in (C), extracellular BPB was washed out (broken line), inducing quick recovery of VAMP-EGFP fluorescence on the plasma membrane. Arrows denote similar amounts of quenching and dequenching of surface fluorescence. When the neurons were restimulated in the absence of BPB, fluorescence rose further, reflecting recovery of EGFP fluorescence as BPB left vesicle lumen. The slow phase of fluorescence recovery after BPB washout might be attributable to spontaneous fusion whose frequency would be temporarily increased after extensive stimulation. Average data (without SEM) from a representative experiment; n = 51 boutons. (E) Concentration-quenching curve obtained on axonal plasma membrane (filled circles, EGFP-outside); n = 120 regions of interest (five coverslips). Smooth curve: IC_{50} = 0.26 mM, n_H = 1.15. No fluorescence loss in HEK293 cells expressing EGFP fused to the cytoplasmic aspect of α_{1C} (open circle, EGFP-inside). n = 89 regions of interest (two coverslips). (F) Schematic illustrating how full reporting of vesicle first fusion can be empirically verified. (G) Experimental tests as sketched out in (F). No differences in quenching time courses obtained with 2 and 3 mM BPB, with either 30 Hz (black) or 1 Hz stimulation (orange). Black triangles represent fluorescence data in the presence of 2 mM BPB but without any stimulation (after photobleaching correction). n = 111–294 boutons (three to six coverslips). In (E) and (G), data points represent mean ± SEM. Many of the SEM bars were smaller than the symbols.

extension, the vesicle membrane, do not display high-affinity binding sites for BPB.

We used FM4-64 to test the effect of VAMP-EGFP expression on vesicle recycling (Figure S3B). Destaining kinetics were no different in VAMP-EGFP-positive or -negative boutons, suggesting that VAMP-EGFP expression had no effect on vesicle recycling.

Verifying that Quenching of VAMP-EGFP by BPB Reflects Kinetics of Vesicle First Fusion

BPB quenching of VAMP-EGFP provided a potentially rigorous way to measure how rapidly vesicles undergo fusion for the first time following initiation of continuous stimulation. This would not be difficult for vesicles undergoing full-collapse fusion but is less confidently

predicted if fusion is followed by rapid retrieval. The FM1-43 destaining curve does not accurately register first fusion because FM dye is partially retained in vesicles after initial fusion events (Figure 1). In contrast, a reliable index of first fusion should fully register fluorescence signals from fresh vesicles, but not from vesicles undergoing second or even later rounds of fusion (Figure 2A).

The key question with BPB is whether intravesicular [BPB] rises sufficiently to cause near-complete quenching before continuity between the external milieu and the vesicle lumen is cut off. We tested this empirically, by increasing [BPB] beyond 2 mM, a concentration sufficient to extinguish almost 100% of EGFP fluorescence (Figure 2E). If fusion pores closed quickly after first opening,

forestalling complete quenching until they had opened multiple times, raising the BPB concentration would result in a more severe loss of fluorescence (red shading, Figure 2F, right). But if fusion pores stayed open long enough after initial opening to allow full quenching, an increase in external [BPB] would produce no greater quenching and no change in the trajectory of fluorescence drop (Figure 2F, left). These scenarios were tested by comparing the quenching with 2 and 3 mM BPB, always referring the data to the TRP (Figure S4A). No significant differences in kinetics were ever observed at either 1 or 30 Hz (Figure 2G). These experiments indicated that the time course of EGFP quenching with 2 mM BPB faithfully reflected the kinetics of first fusion events, be they full-collapse or rapid retrieval.

This method for tracking first fusion complements an approach wherein first fusion is registered by the escape of intravesicular H^+ and the unquenching of synaptopHluorin (Fernandez-Alfonso and Ryan, 2004; Sankaranarayanan and Ryan, 2001). The two methods make significantly different use of bafilomycin A1. In the synaptopHluorin-H^+ method, neurons are pretreated with bafilomycin A1 for 30–60 s, with the rationale that this will completely inhibit the vesicular H^+ pump but spare the vesicles' initial acidity. This relies on striking a delicate balance and is open to uncertainty about whether the H^+ pump was completely blocked. In the BPB method, complete loss of the pH gradient was achieved with >1 hr bafilomycin A1 pretreatment and confirmed experimentally (Figure S2B).

Contrasting Kinetics of VAMP-EGFP Quenching and FM1-43 Destaining over a Wide Range of Stimulus Frequency

BPB quenching of VAMP-EGFP allowed us to study how vesicle first fusion kinetics varied with the frequency of stimulation. As stimulation rate was raised from 0.3 to 30 Hz, EGFP quenching became increasingly rapid (Figure 3A). The half-time for extinction of the EGFP fluorescence decreased from >5 min to ~12 s, consistent with speedier recruitment of fresh vesicles.

Figure 3B shows the time course of FM1-43 destaining evoked by the same set of stimulation frequencies. For every one of the 1379 boutons in this study, fluorescence signals were referred to the size of the TRP (Figures 1G and 1H for FM1-43, and Figure S4A for VAMP-EGFP). At each frequency, the fractional drop in fluorescence was consistently smaller for FM dye than for BPB quenching of VAMP-EGFP (e.g., 1 and 10 Hz, Figures 3C and 3D). The clear kinetic differences confirm that vesicles were not generally able to discharge their entire FM dye content upon first fusion, in agreement with Figure 1.

The rates of VAMP-EGFP quenching and FM1-43 destaining were different from the very beginning of stimulation. The slope of the VAMP-EGFP quenching curve reflected the probability density function (PDF) for first fusion events (Figure 3E, thick lines; same curves overlaid without normalization in Figure 4A1). At 0.3 Hz, the rate of first fusion peaked immediately after stimulation began, reaching ~0.36% s^{-1}, then fell slowly as the pool of unquenched vesicles was gradually depleted over several minutes. At 30 Hz, the rate of first fusion reached 6.8% s^{-1} before falling steeply in tens of seconds. In comparison with the kinetics of first fusion, the initial rate of FM1-43 destaining (thin lines) was lower at every frequency (Figure 3E, arrowheads). The difference in initial slopes was 10-fold at 0.3 Hz and waned gradually with increasing stimulus frequency (Figure 3F). Even at 30 Hz, the difference remained as large as ~2-fold, far from the expected ratio of 1 if only full-collapse fusion had been involved.

The rate of FM1-43 destaining decayed slowly enough to cross the rate of first fusion (arrows in Figure 3E mark t_{cross}). The higher the stimulation frequency, the earlier the intersection (t_{cross}^{-1} plotted versus frequency in Figure 3G). Beyond the crossing, FM1-43 destaining proceeded at a more rapid rate than first fusion, implying that some vesicles were providing a delayed release of dye even after they had already fused for the first time.

Inferences about Individual Vesicle Behavior, Averaged over the Recycling Pool

Figure 4A superimposes the curves describing the probability of first fusion per unit time (Figure 3E), all plotted with the same axes. This kinetic information provides a starting point for extracting the behavior of individual vesicles, using an analysis illustrated in Figure 4B. The fluorescence loss of a bouton (Figure 4B3) is the sum of the fluorescence losses of individual vesicles. This can be approximated by repeatedly adding a general description of single vesicle behavior, time-shifted according to various individual time delays to first fusion (Figure 4B2). The overall bouton destaining would thus be predicted by convolving the first fusion probability (Figure 4B1) with the average single vesicle fluorescence response (SVFR). Conversely, deconvolution can be used to derive the average SVFR for individual vesicles (Figure 4B2) from the first fusion probability (Figure 4B1) and overall bouton fluorescence loss (Figure 4B3). The SVFR is generated by the first fusion and later repeated fusions in combination. This analysis does not require that each single vesicle destains with exactly the same unitary kinetics, but only assumes that the SVFR does not systematically vary with the time delay to first fusion. This assumption was directly supported by the finding that single vesicles stained with FM1-43 displayed virtually identical destaining trajectories regardless of whether the first fusion occurred relatively early or late during the course of stimulation (Figure S5).

A family of average SVFRs at various stimulation frequencies was derived by numerical deconvolution from our experimentally determined data (Figure 4A2). At all frequencies, the SVFRs were slower and kinetically richer than the sudden down step to zero expected for classical full-collapse fusion alone. The SVFRs included a rapid initial drop, but the sudden fluorescence loss was only partial. In each case, the SVFR continued to fall to a lower level, presumably due to repeated fusions occurring at variable intervals after the time-aligned first fusion.

As a limiting case, one may attribute all of the rapid initial drop to vesicles undergoing full collapse. This is clearly an extreme assumption because part of the initial fluorescence loss would originate from vesicles undergoing kiss-and-run (Aravanis et al., 2003a). In this way, the size of the initial drop provided an upper limit on the relative extent of full-collapse fusion. These limits ranged from <20% at 0.3 Hz to ~50% at 30 Hz (Figure 4C).
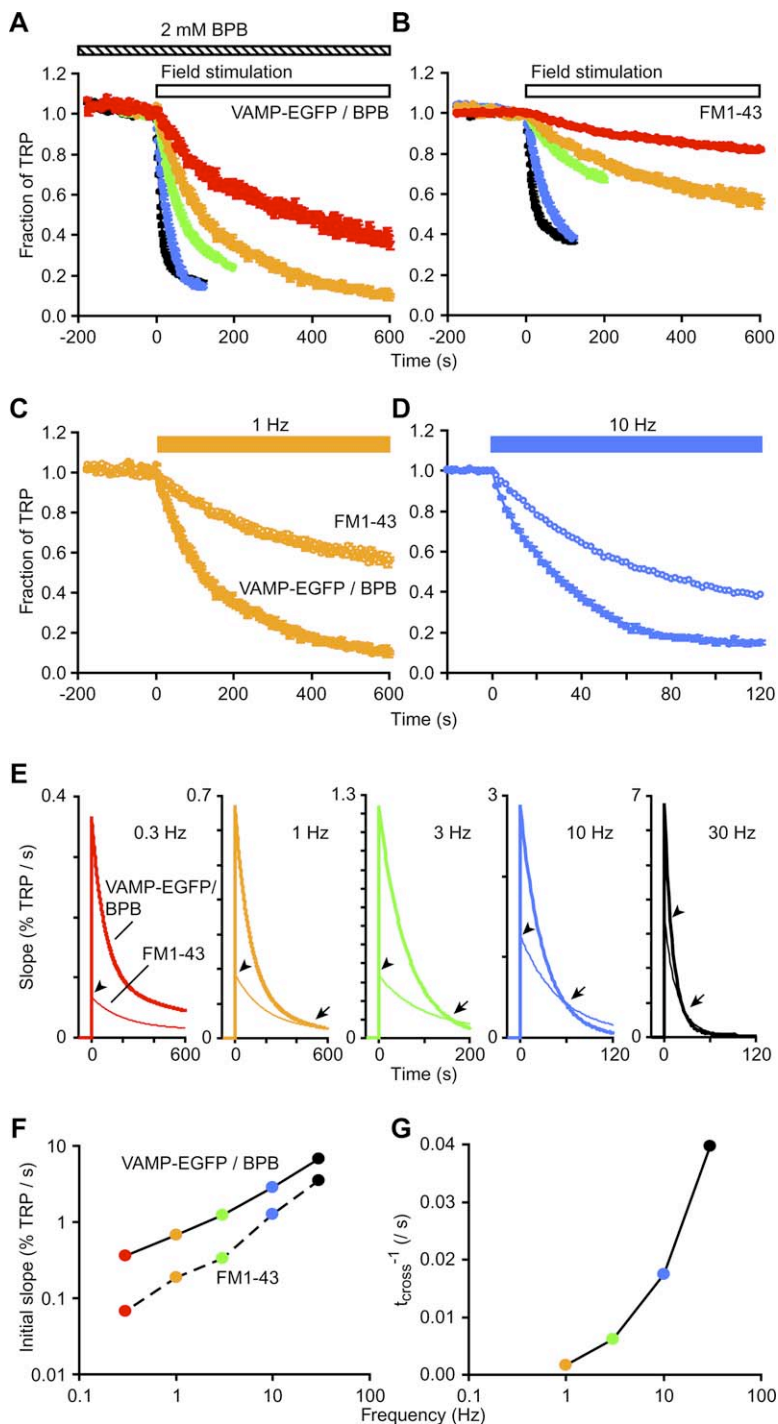
Figure 3. Fluorescence Loss by First Fusion Was Consistently Greater than FM1-43 Destaining at Various Stimulation Frequencies

(A) Changes in VAMP-EGFP fluorescence plotted against time. Time course of first fusion (with 2 mM BPB) was frequency dependent. 30 Hz, black; 10 Hz, blue; 3 Hz, green; 1 Hz, orange; 0.125 Hz, red (same color-coding of frequency in other figures). n = 221–562 boutons (three to ten coverslips). (B) Time course of FM1-43 destaining was also frequency dependent. n = 110–545 boutons (four to ten coverslips). (C and D) Overlays of first fusion time course (VAMP-EGFP quenching in 2 mM BPB, closed circles) and FM1-43 destaining (no BPB, open circles), with stimulation at 1 Hz (C) or 10 Hz (D). First fusion kinetics were much faster than FM1-43 destaining. y axes in (A)–(D) represent fractions of TRP, for appropriate comparison between fluorescence signals. In (A)–(D), data points represent mean ± SEM. Many of the SEM bars were smaller than the symbols. (E) Slopes of the fluorescence intensity curves (such as those in [A] and [B]) at different stimulation frequencies. At every frequency, first fusion (thick line) showed greater peak slope than FM1-43 destaining (thin line). Arrowheads point to initial slopes of FM1-43 destaining. Arrows point to intersections between the two curves, indicating the time when FM1-43 destaining became faster than first fusion. (F) Initial slopes of first fusion (continuous line) and FM1-43 destaining (broken line) plotted against stimulation frequency. (G) Time of intersection of first fusion and FM1-43 destaining curves, expressed as a reciprocal, plotted against stimulation frequency.

The progressive decay of SVFR after the initial drop is an indication of further dye loss due to rounds of fusion subsequent to the first exocytotic event (vesicle reuse). Individual vesicles would be expected to show a series of abrupt down steps at various delays over the period of stimulation (Aravanis et al., 2003a, 2003b). However, averaged across the population of recycling vesicles, the later down steps would smooth out to a gradual decay. The initial slope of the decay increased with stimulation frequency, as expected for a greater incidence of renewed exocytotic events per unit time. The magnitude of the initial slope rose from ~0.001 s^{-1} at 0.3 Hz to 0.013 s^{-1} at 30 Hz, a 14-fold acceleration (Figure 4D). This frequency dependence reflects changes in delays between first and later fusion events and in the balance between full-collapse fusion and kiss-and-run, ensemble-averaged over the entire population of vesicles.

Another notable feature of the SVFRs was the nonzero steady-state level after the roughly exponential decay phase had settled, ranging from 0.69 at 0.3 Hz to 0.19–0.24 at 10–30 Hz (Figure 4A2). A possible interpretation is that continuous stimulation drives some of the
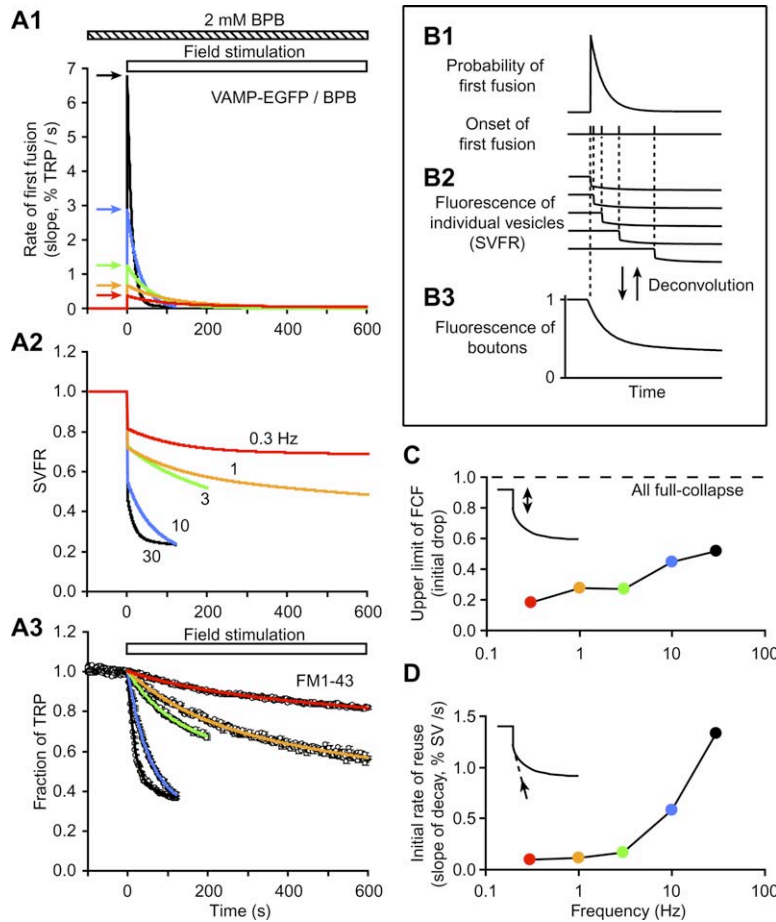
Figure 4. Vesicle Fusion and Recycling Modes Studied by Deconvolution

(A) Deconvolution analysis. The averaged first fusion and FM1-43 destaining curves (Figures 3A and 3B) were fit with double exponential functions. The closeness of the fits are shown in (A3). The rate of first fusion (A1) was calculated as the derivative of the smooth curves. The arrows in (A1) indicate wide range of peak rates. Curves in (A1) and (A3) were used for numerical deconvolution to calculate single vesicle fluorescence responses (SVFRs) at various frequencies (A2).
(B) Schematic illustration of principle of deconvolution analysis.
(C) Frequency dependence of upper limit on full-collapse fusion (FCF), based on the initial drop in SVFR.
(D) Frequency dependence of initial rate of reuse, measured as the initial slope of the decay phase in SVFR (A2).

boutons into states of Ca^{2+} channel inactivation (Xu and Wu, 2005) or release inactivation or unavailability (Hsu et al., 1996). Similar processes may have limited the amount of first fusion itself (Figure 3A). Presumably, the release mechanism regains responsiveness only after a quiescent period before the next bout of stimulation. The graded, frequency-dependent decrease of the steady component conformed to the expectation that the higher the frequency, the more vigorously vesicles are recruited.

Evidence for Kiss-and-Run Fusion and Reuse without Reliance on FM Dye

So far, our evidence for kiss-and-run in small nerve terminals has relied on experiments with FM1-43. To test for nonclassical fusion/retrieval and reuse without using FM dye, we sought additional kinetic perspective from experiments with low [BPB]. As shown in Figure 5A, the rationale was to seek a condition in which the delay between fusion and retrieval was too brief to allow steady-state quenching to be achieved with single events. Weaker quenching at low [BPB] would create a transitory discrepancy with the more severe quenching at high [BPB] (red shading, Figure 5A, right) (the converse of Figure 2H). Indeed, the time course of quenching by 0.3 mM BPB was significantly slower than that found with 2 mM BPB (Figure 5B, open and closed symbols). In both cases, the fluorescence scale was referred to the TRP but not further scaled. The marked difference

in the time courses of fluorescence loss was not consistent with full equilibration during first fusion. Instead, it indicated the participation of nonclassical exo-endocytosis. The averaged behavior of individual vesicles was derived by deconvolution (Figure 5C). The average SVFR consisted of an immediate but partial drop of fluorescence, followed by a further gradual decay (Figure 5C2), similar to the SVFR with FM1-43 (Figure 4A2). For additional perspective, we performed deconvolution analysis on the time course of FM1-43 destaining in the presence and absence of 2 mM BPB (Figure 1F) and obtained a very similar result.

Table 1 shows a comparison among different methods of BPB quenching, all at 30 Hz. In every case, there was an initial drop in the SVFR, indicating an upper limit on full-collapse fusion (44%–52% of first fusion), and a slow relaxation (half-time of reuse of 9.8–18.2 s). The degree of agreement was reasonably good, given the use of waveforms based on population studies. The similarity in SVFR parameters reinforced the conclusions that kiss-and-run coexisted with full-collapse fusion and that vesicles underwent reuse after first fusion.

Pulses of Surface Quenching Provide a Lower Limit on Classical Full-Collapse Fusion

Brief applications of quencher gave us the means to set a *lower* limit on the proportion of fusion events that take place by full-collapse fusion. A hallmark of full-collapse fusion is the persistent exposure of vesicle proteins
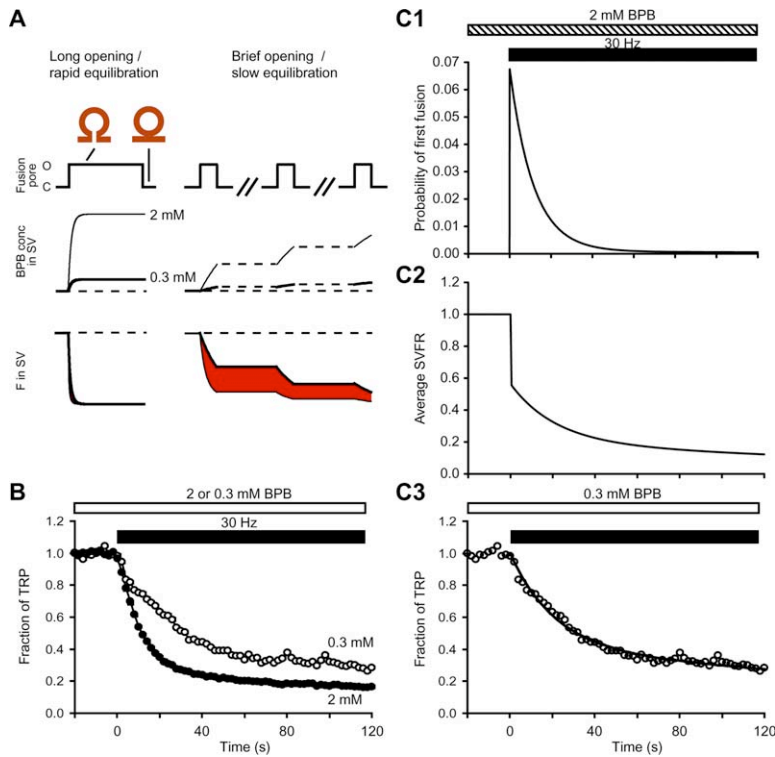
Figure 5. Probing for the Presence of Kiss-and-Run Using VAMP-EGFP with Different Concentrations of BPB

(A) Schematic illustrating fluorescence changes with low and maximally effective concentrations of quencher for two scenarios: fusion pore openings outlasting equilibration of BPB within vesicles (left), and openings too brief to allow BPB equilibration (right). See text for details.

(B) VAMP-EGFP quenching by 2 mM (filled circles) and 0.3 mM BPB (open circles). Data for 2 mM BPB was the same as in Figure 3A. n = 452 boutons (six coverslips for 0.3 mM BPB). The SEM bars were smaller than the symbols.

(C) Deconvolution analysis. The curve of first fusion rate (C1) was obtained as in Figure 4A1. The curve with 0.3 mM BPB was fit with a double-exponential function (C3). These curves were deconvolved to calculate the SVFR (C2).

on the neuronal surface after vesicles have fused completely with the plasma membrane (Gandhi and Stevens, 2003; Li and Murthy, 2001; Sankaranarayanan and Ryan, 2000). Thus, full-collapse fusion might be monitored as an increased surface accessibility of VAMP-EGFP, detectable by a brief exposure to BPB (Figure 6). In this protocol, a pulse of BPB was applied before any stimulation to define the basal level of surface VAMP-EGFP. An identical pulse of BPB, applied ∼18 s after extensive field stimulation, was accompanied by a significant increase in quenching, reflecting increased VAMP-EGFP on the plasma membrane. After a rest period of ∼5 min, a third pulse of BPB showed that the increment in surface quenching had fully reversed; evidently, the extra VAMP-EGFP had been completely reinternalized through endocytosis. The temporary increment in surface quenching after field stimulation averaged 38.1% ± 0.7% of the TRP, which was later defined in the individual boutons (Figure 6, right). The increment was fully attributable to full-collapse fusion because the ∼18 s interval between ces-

sation of stimulation and the onset of the BPB pulse was several-fold longer than conservative bounds on the time required for rapid retrieval of vesicles undergoing kiss-and-run (Aravanis et al., 2003b; Gandhi and Stevens, 2003). The estimated lower bound (38%) helps delimit the extent of full-collapse fusion, taken together with the upper bound derived from deconvolution (∼50%).

Initial Probability of Release and Its Dependence on Stimulation Frequency

The initial slope of the first fusion time course (Figure 3A) contains valuable information about the initial release probability of nerve terminals (P_r) before significant vesicle depletion had occurred. When ensemble fluorescence signals were replotted against stimulus number, the initial slopes showed a striking inverse dependence on stimulation frequency (Figure 7A; see Supplemental Experimental Procedures for details). When the initial slopes were expressed in absolute units, to describe initial vesicle release rates in the same terms as the P_r of

Table 1. Comparison of Average SVFR

Fast (first fusion)	VAMP-EGFP + BPB (2)[a]	FM1-43 + BPB (2)	FM1-43 + BPB (2)	VAMP-EGFP + BPB (2)
Slow	FM1-43	FM1-43 (population)	FM1-43 (individual boutons)	VAMP-EGFP + BPB (0.3)
Initial drop (upper limit on FCF)	0.517	0.515	0.44 ± 0.011 (0.421)[b]	0.438
Half time of slow decay (s)	12.6	9.8	9.6 ± 0.4 (9.0)	18.2
Steady-state	0.242	0.025	0.136 ± 0.010 (0.141)	0.128

FCF, full-collapse fusion. All experiments were done with 30 Hz stimulation. The data in columns correspond to experiments in Figures 4, 1, 8, and 5, respectively.
[a]Parenthesis after BPB indicates concentration (in mM).
[b]Statistical data in parentheses were obtained from averaged FM1-43 destaining curves with and without BPB.
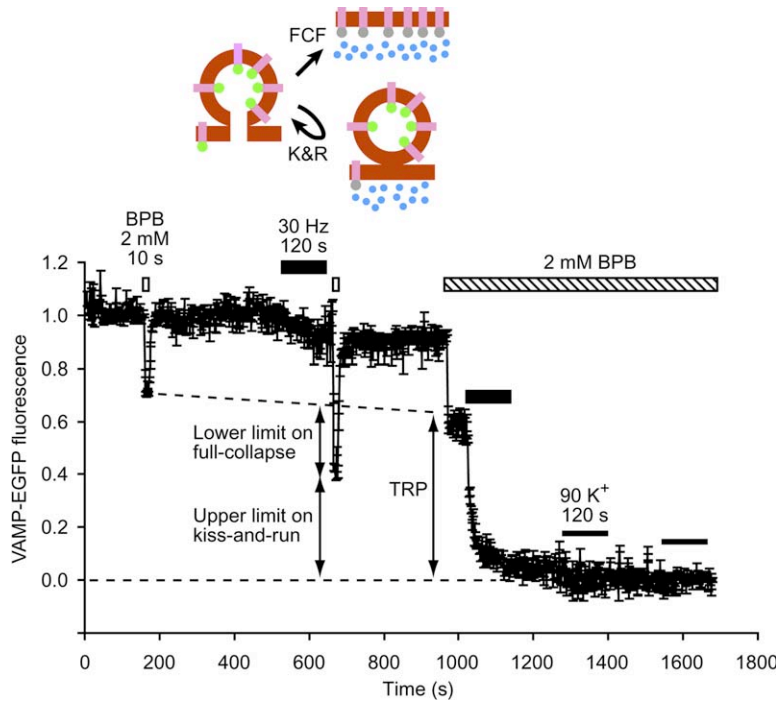
Figure 6. Use of Surface Quenching to Set a Lower Limit on the Extent of Full-Collapse Fusion

(Top) Schematic diagram illustrating the incremental exposure of vesicular VAMP-EGFP to extracellular BPB lingering after full-collapse fusion, but not after kiss-and-run. (Bottom) VAMP-EGFP on plasma membrane was quenched by two applications of BPB (2 mM, 10 s), one before field stimulation and another 18 s after the end of field stimulation (30 Hz for 120 s). After a rest period, a third BPB application produced surface quenching whose magnitude had recovered to prestimulus level (dotted line). Additional field stimulation and subsequent 90 mM K^+ challenges were used to define TRP size. Average of data from 304 boutons (three coverslips) with SEM bars (data symbols omitted for clarity). The lower limit on full-collapse fusion was calculated as 38% based on the bracketing control responses (dotted line). Note that the conditions in this experiment (120 s stimulation, 18 s recovery) differ markedly from those in Figure 2C (40 s stimulation and 60 s recovery), which likely allowed recovery of newly surface-exposed VAMP-EGFP).

quantal neurotransmission, they showed a wide and skewed distribution at all stimulation frequencies (Figure 7B, top), and a correlation with TRP size (Figure 7B, bottom).

Figure 7C shows cumulative distributions of the initial slopes of fluorescence loss, plotted as initial P_r (top axis) as well as fluorescence a.u. per AP (bottom axis). The median value of P_r increased progressively as the stimulation frequency was lowered from 30 Hz to 0.3 Hz. Interestingly, in ~15% of the nerve terminals, the initial slope at 0.3 Hz was greater than one per AP, reaching values as high as >4 vesicles per AP. In the great majority of boutons, however, <1 vesicle was released during single excitations. The findings with BPB are qualitatively similar to, but quantitatively different from previous studies with FM1-43.

Evidence for Kiss-and-Run in Individual Boutons
All of the analysis so far was performed on averaged data, obtained from a large population of boutons, cultured on multiple coverslips. The results can be explained by two different scenarios. In one case, individual boutons exhibit mixtures of kiss-and-run and full-collapse fusion with some variability. In another scenario, individual boutons engage in either kiss-and-run or full-collapse fusion, but not both, and the bimodal behavior is an attribute of the population of terminals. Additional experiments tested which of these scenarios holds true and explored whether the prevalence of fusion modes varies with P_r, as reflected by the initial slope of fluorescence loss in the presence of BPB (Figure 7). We returned to the use of BPB quenching of FM1-43, measuring FM1-43 destaining twice, first in the absence
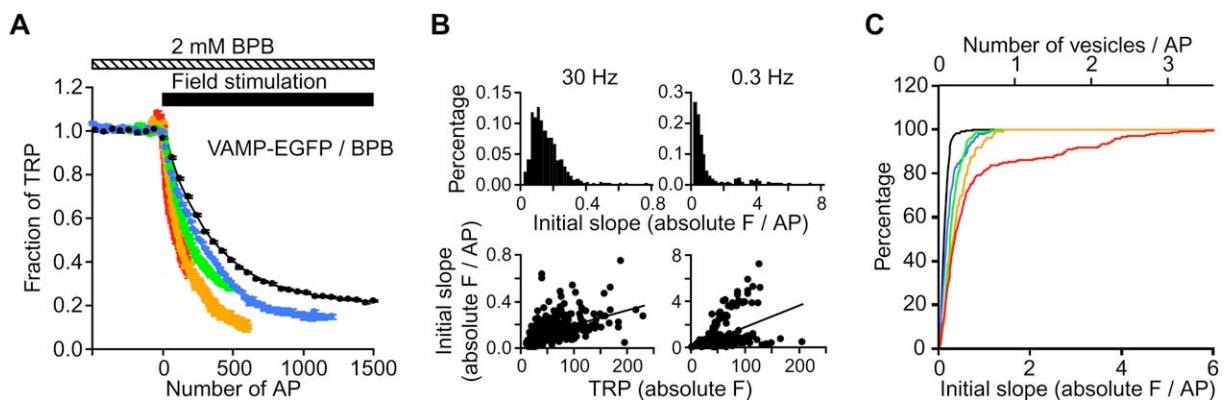
Figure 7. Initial Probability of Vesicle Fusion (P_r) in Individual Boutons Derived from the Measured Rate of Vesicle First Arrival

(A) Plot of the VAMP-EGFP quenching data against the number of action potentials (AP). Data points represent mean ± SEM. Many of the SEM bars were smaller than the symbols.
(B) Distribution of initial rates of first fusion (top) and their correlation with the TRP size (bottom) at 30 (left) and 0.3 Hz (right).
(C) Cumulative plots of vesicles per AP (nominal initial P_r) at different stimulation frequencies.
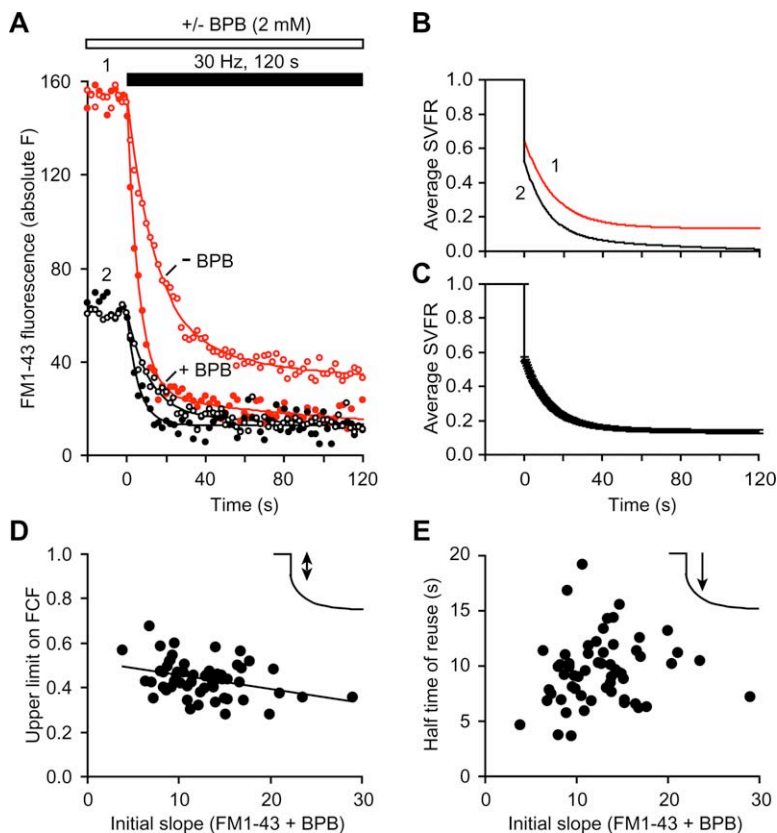
Figure 8. Testing for the Presence of Kiss-and-Run in Individual Boutons

(A) FM1-43 destaining curves from two exemplar boutons (denoted in red and black) in the presence (filled circles) and absence of 2 mM BPB (open circles). y axis: absolute FM1-43 fluorescence intensity, with zero corresponding to the level after three rounds of 90 mM K^+. Differing initial values reflect the absolute sizes of the TRP. Continuous curves: double exponential fits. (B) SVFRs calculated by deconvolution from corresponding curves in (A). The initial drop (upper limit on full-collapse fusion) was smaller for bouton 1, which showed the larger TRP size (A), illustrating a trend shown in (D). (C) Pooled data of SVFRs from 58 boutons in a single experiment. Bars represent SEM. (D) Upper limit on full-collapse fusion, plotted against the initial slopes in the presence of BPB (reflecting initial P_r). Regression analysis shows significant correlation (r = 0.350; p < 0.01; n = 58). (E) Half-time of reuse, plotted against the initial slopes in the presence of BPB. No significant correlation (r = 0.139; p > 0.1; n = 58).

of quencher and later in the presence of 2 mM BPB (Figure 8). This allowed us to derive key parameters of vesicle first fusion, retrieval, and reuse in single nerve terminals. Figure 8A illustrates results from two representative boutons. The y axis shows the absolute intensity of FM1-43 fluorescence, with the zero level empirically determined by three rounds of 90 mM K^+. The differing initial values reflected variability of TRP size. In both exemplar boutons, FM1-43 destaining was significantly hastened by BPB. Deconvolution analysis, performed one bouton at a time, produced qualitatively similar SVFR waveforms, consisting of an initial drop followed by a smooth decay (Figure 8B). The average of the individual SVFRs (n = 58; Figure 8C) agreed well with the SVFR obtained by a single deconvolution of aggregate FM destaining curves in the presence and absence of BPB (Table 1). The agreement validated the approach of using averaged signals.

We looked for quantitative differences and trends among individual boutons (Figures 8D and 8E). For example, the SVFR showed a smaller initial drop for bouton 1 (0.35) than for bouton 2 (0.47). The initial drop (upper limit on full collapse) averaged 0.440 ± 0.011 (n = 58 boutons) and showed a significant negative correlation with our index of P_r (p < 0.01). Thus, the higher the initial P_r, the more restricted the upper bound on full collapse and the greater the possibility of kiss-and-run. In the same set of 58 boutons, the half-time of reuse averaged 9.55 ± 0.40 s. The $t_{1/2}$ for reuse displayed a wide variability, and no significant correlation with the index of P_r (p > 0.1, Figure 8E). The SVFR settled at a nonzero steady level in most boutons, averaging 13.6% ± 1.0%. In summary, the great majority of nerve terminals dis-

played the ability to support kiss-and-run, even at 30 Hz, the stimulation frequency at which full-collapse fusion appeared most prominent.

Discussion

Several properties of the quencher BPB proved advantageous for probing fusion properties at synapses between CNS neurons. BPB quenches VAMP-EGFP and FM1-43, widely used fluorophores for studying synaptic vesicle recycling, in contrast to H^+ ions, which quench GFP-based indicators such as synaptopHluorin, but not FM dyes. Like the fast neurotransmitters glutamate and GABA, BPB is a hydrophilic, negatively charged small molecule that takes the aqueous route connecting the vesicle to the external milieu. BPB uptake and loss can be monitored without confounding effects of intrinsic transport across the vesicle membrane, a concern for H^+ quenching of GFP-based indicators, which relies on block of H^+ transport without loss of H^+ gradient. BPB quenching was reversible, both on the plasma membrane and in vesicles, and had no adverse effects on vesicle recycling. The concentration of BPB could be raised to millimolar levels, high enough to reach an empirical ceiling on the rate of fluorescence quenching.

Capitalizing on these favorable characteristics, we have shown that the recycling pool of vesicles is capable of engaging a mode of exo-endocytosis distinct from classical full-collapse fusion, termed kiss-and-run. This nonclassical mode is here defined operationally as a transient fusion event in which transfer of probe molecules between vesicle lumen and extracellular space is hindered. The ability to support kiss-and-run and vesicle

reuse without loss of identity extended to the TRP, not just the vesicles already residing in the RRP for some time before stimulation. Variations in stimulation frequency modified the rate of first fusion, the balance between kiss-and-run and full-collapse fusion, and the kinetics of vesicle reuse, with important implications for the bandwidth of synaptic information transfer.

Use of BPB to Delineate First Fusion Kinetics and Initial P_r

Detailed kinetic analysis of the vesicle cycle is extremely challenging, in part because of the complexity of its cell biology (Jahn et al., 2003; Murthy and De Camilli, 2003; Slepnev and De Camilli, 2000; Sudhof, 2004). Upon stimulus initiation, individual vesicles vary greatly in physical starting location and biochemical status. By focusing on a pivotal event, first-time fusion, we were able to separate events leading up to this kinetic watershed (e.g., the initial translocation, docking, and priming) from processes following it (e.g., vesicle retrieval, repriming). The delay to first fusion was monitored cumulatively as the fluorescence change arising from BPB quenching of VAMP-EGFP. Control experiments at two different levels of [BPB] verified that the first fusion kinetics had been accurately determined. At a sufficiently high concentration (2 mM), the initial rates of BPB quenching of EGFP or FM1-43 were similar, agreeing within 14%. Optical recordings provided different information than that gleaned from typical electrophysiological recordings inasmuch as many individual synapses were studied simultaneously, but each vesicle was counted only once (see also Sankaranarayanan and Ryan, 2001). The use of BPB led to two main conclusions. First, we saw initial slopes of fluorescence loss corresponding to initial P_r values that were at least 2-fold higher than those suggested by FM1-43 destaining under the same conditions (Figures 3A and 3B). Second, we found that a small fraction of vesicles could not be accessed over the course of a single bout of continuous stimulation, suggesting that vesicle mobilization was limited by exocytotic adaptation (Hsu et al., 1996) or Ca^{2+} channel inactivation (Xu and Wu, 2005), processes that could be removed during a rest period before further stimulation.

Upper and Lower Limits to the Prevalence of Full-Collapse Fusion

We obtained several pieces of evidence that excluded the idea that classical full-collapse fusion was the sole means of exocytosis at synapses between cultured hippocampal neurons. First, FM1-43 was retained in vesicles well after they had undergone first fusion as shown definitively by BPB quenching of trapped intravesicular FM1-43 (Figures 1E, 1F, and 8) (see also Kavalali et al., 1999; Klingauf et al., 1998; Pyle et al., 2000). Second, FM1-43 destaining lagged behind first fusion as defined by BPB quenching of VAMP-EGFP (Figures 3A–3D and 4), whereas their time courses should have agreed to within 1–2 sampling intervals (<2–4 s) if classical full-collapse fusion had been the only operative mechanism of exocytosis. Third, the time course of fluorescence loss was slowed significantly by reducing the [BPB], in contrast to the near-identical kinetics expected if there had been complete equilibration at each quencher concentration, as expected for classical fusion.

Each of the various experimental approaches offered special advantages. The study of FM destaining in the absence and presence of BPB lent itself to an analysis of individual nerve terminals because FM destaining could be performed repeatedly in the same boutons (Figure 8). The quenching of VAMP-EGFP provided the most rigorous information on first fusion kinetics inasmuch as the source of fluorescence was fixed to the vesicle lumen. The use of submillimolar [BPB] avoided the use of FM dyes completely but relied instead on the progressive accumulation of quencher with repeated fusions as the indicator of reuse. The various methods provided similar upper limits on the fraction of exocytotic events that took place by classical full-collapse fusion at 30 Hz (0.52, 0.52, 0.44, respectively). These upper limits on full-collapse fusion were complemented by an estimated lower bound, 0.38, derived from incremental surface quenching (Figure 6). In sum, these experiments reinforce the conclusion that kiss-and-run must coexist with full-collapse fusion.

Participation of Kiss-and-Run Generalizes across Nerve Terminals, Vesicle Pools, Temperatures, and Stimulation Frequencies

The participation of kiss-and-run was found to be general across a wide range of circumstances. The FM + BPB experiments (Figure 8) demonstrated that virtually all boutons, not just a particular subset, engaged in nonclassical fusion/retrieval. With regard to vesicle pools, the large degree of nonclassical exo-endocytosis (>50%) precluded the hypothesis that it was restricted to vesicles basally positioned in the RRP (<20%–30% of TRP) (Pyle et al., 2000). With regard to temperature, we found that at ~33°C, FM1-43 destaining kinetics were accelerated by BPB (Figure S1B), just as at ~23°C (Figure 1F), indicating involvement of kiss-and-run at warmer temperature. Finally, the incidence of kiss-and-run became more predominant the lower the stimulation rate, increasing from ~50% at 30 Hz to >80% at 0.3 Hz (Figure 4C).

Kiss-and-Run Allows Vesicle Retrieval to Keep Pace with Exocytosis at Low to Moderate Frequencies

Finding that the prevalence of kiss-and-run is frequency dependent imposes important limitations on the ability of nerve terminals to keep their vesicle membrane internalized, thus avoiding drastic perturbation of their morphology. Kiss-and-run events are associated with a much briefer connection between vesicle lumen and extracellular milieu than classical full-collapse fusion (Aravanis et al., 2003a; Gandhi and Stevens, 2003; Richards et al., 2005). Therefore, the greater the preponderance of kiss-and-run, the smaller the percentage of time that vesicle membrane is externalized. By showing that the balance is increasingly tipped in favor of kiss-and-run, the lower the stimulation frequency, our experiments predict that the ability of vesicle retrieval to keep up with exocytosis will vary strongly with stimulation frequency. This expectation fits well with observations of Fernandez-Alfonso and Ryan, who showed clearly that accessibility of synaptopHluorin to external H^+ was restricted at low to moderate frequencies (Fernandez-Alfonso and Ryan, 2004). We agree with their suggestion that "…endocytosis operates intrinsically at a fast rate,

in the sense that it balances exocytosis effectively to prevent significant depletion of the releasable pool of vesicles onto the presynaptic surface during robust synaptic activity." They suggested that this could be taken as evidence that kiss-and-run operates continuously during repetitive AP firing (our view also) but pointed out two aspects of their data that appeared inconsistent with preexisting definitions of kiss-and-run. One feature was that most of the TRP participates in the exo-endocytotic process during continuous repetitive AP firing. This is no longer an impediment to reaching consensus about the basis of exo-endocytotic balance, inasmuch as our experiments now support the idea that the entire recycling pool participates in kiss-and-run.

Another issue (and the locus of possibly remaining disagreement) was whether FM dyes destain with kinetics different from that predicted by full-collapse fusion. Fernandez-Alfonso and Ryan contended that synaptic vesicles loaded with FM dye lost all fluorescence upon first fusion, based on an experiment where both FM4-64 destaining and synaptopHluorin quenching were ~80% complete after a bout of 5 Hz stimulation (Fernandez-Alfonso and Ryan, 2004). We see two problems with this experiment. The first is an internal contradiction. Midway during the 5 Hz stimulation, only 30%–40% of the recycling pool had fused according to synaptopHluorin method, but 60%–70% according to FM4-64 destaining (Fernandez-Alfonso and Ryan, 2004). This result is problematical because it is physically impossible for first-fusing vesicles to lose more than 100% of their FM dye. The second problem concerns the protocols used to pin down the size of TRP. Fernandez-Alfonso and Ryan assume that two or three rounds of field stimulation were enough to fully destain the TRP, whereas we find that, even after multiple rounds of field stimulation, further stimulation with 90 mM K$^+$, interspersed with rest periods, leads to additional destaining (Figure S4B). Incomplete destaining of FM dye would lead to underestimation of the TRP and an overestimation of the speed of FM destaining. Despite these remaining experimental differences, our experiments and those of Fernandez-Alfonso and Ryan complement each other in showing the frequency dependence of rapid endocytosis and its importance for exo-endocytotic balance.

SVFR and the Rapid Time Course of Vesicular Reuse

The process of deconvolution provided a kinetic representation of how single vesicles behaved once they had fused for the first time. The power of this kind of mathematical approach is exemplified by biophysical analysis of voltage-dependent Na$^+$ channels, which separated the latency to first opening from the kinetics of inactivation after first opening (Aldrich et al., 1983). In our analysis, the SVFR describes ensemble behavior, averaged across all vesicles once they have fused, including vesicles whose first fusions occurred at various stages during the stimulus train. Progressive changes in the SVFR over the course of the ongoing stimulation could be neglected as a first approximation, based on direct observations of individually stained vesicles (Figure S5).

Reassuringly, each of our approaches led to a similar SVFR. The deconvolution analysis generated SVFR with a strikingly biphasic time course at frequencies between 0.3 and 30 Hz (Figures 4A2, 5C2, and 8C and Table 1). An initial rapid drop signaled the consequences of first fusion and was accounted for by coexisting modes of kiss-and-run and full-collapse fusion. A subsequent decaying tail in the SVFR was also found across all frequencies. The decaying tail lumps together several possible forms of kinetic behavior, including repeated rounds of kiss-and-run (Aravanis et al., 2003a, 2003b; Pyle et al., 2000; Sara et al., 2002), loss of all the remaining dye in a single full-collapse event, and loss of only a portion of dye followed by refractoriness to further release until a rest period has ensued. The stepwise, but stochastic behavior of a large number of vesicles presumably gave rise to a smoothly decaying tail with a characteristic half-time. At 30 Hz, estimates of $t_{1/2}$ ranged from ~10 s (BPB + FM dye) to ~18 s (low and high BPB). The BPB + FM experiments were particularly compelling because each bouton served as its own control, allowing us to derive the time course of reuse in >50 boutons (Figure 8; Table 1). The variation among individual boutons was modest and showed only mild correlation with an index of P_r or with TRP size, consistent with the assumption that boutons and vesicles behave homogeneously enough to allow analysis based on average properties. The mean $t_{1/2}$, 9.6 s, was in good agreement with a half-time of ~10 s estimated from FM destaining of single vesicles with high-frequency stimulation (Aravanis et al., 2003a).

Frequency Dependence of Exo-Endocytotic Cycling and Functional Implications

Frequency-dependent modulation of the vesicle cycle (Sudhof, 2004) has been easier to study at calyceal nerve endings (Wu, 2004) and retinal bipolar terminals (Royle and Lagnado, 2003) than at small central terminals, where the impact on synaptic information transfer would be most critical. We found that stimulation frequency influenced all aspects of vesicle dynamics, not only leading up to first fusion but also following it. During infrequent activity, fusion/retrieval was dominated by kiss-and-run. As stimulation frequency was progressively elevated, we observed multiple changes in vesicle dynamics, which shaped the overall impact of frequency on rates of vesicle turnover. First, the estimated upper limit on the relative contribution of full-collapse fusion increased 2.6-fold between 0.3 (18%) and 30 Hz (52%), suggesting increasing mobilization of classical vesicle recycling with increased frequency. Second, the rate of reuse speeded up 14-fold over the same frequency range, with $t_{1/2}$ decreasing to ~10 s at 30 Hz. Third, the steady component of the SVFR sharply dwindled, as if accommodation of the release machinery (Hsu et al., 1996) was overcome by increased Ca^{2+} entry.

A predominance of kiss-and-run at slow firing rates would be energetically advantageous in keeping vesicle components on vesicles (Taraska et al., 2003; Tsuboi et al., 2000) and would preserve a reservoir of transmitter-filled vesicles in readiness for meeting the demands of intermittent bursts of spikes. The apparent shift away from kiss-and-run with increased frequency seems counterintuitive at first but may be mechanistically determined: rapid vesicular retrieval might require a minimal time for preparation, whereas classical slow retrieval may not. Nerve terminals may resort to full-collapse fusion as a way of getting maximal transmitter

release in a limited period, even if it is less efficient and builds up a debt that must be repaid later, analogous to anaerobic metabolism during extreme exertion.

Taken together, the various effects of stimulus frequency on vesicle dynamics leave ample leeway for a substantial functional role of kiss-and-run over the entire 100-fold frequency range. The 2.6-fold increase in the upper bound on full-collapse fusion is outweighed by the 14-fold speeding of reuse. Thus, kiss-and-run events will still outnumber full-collapse fusions. Another perspective is provided by consideration of the initial drop in the SVFR, $\sim$50% at 30 Hz. Accordingly, the $t_{1/2}$ of the subsequent relaxation provides a rough estimate of the delay between first fusion and further loss of an equivalent fraction of the remaining fluorescence (one cycle of vesicular reuse). The observed $t_{1/2}$ of $\sim$10 s is long enough to allow neurotransmitter replenishment (Pyle et al., 2000; Zhou et al., 2000) but is much shorter than the several tens of seconds required for complete recovery from full-collapse fusion, a significant kinetic advantage.

Experimental Procedures

Cell Culture and Solutions
Cultured hippocampal neurons were obtained from CA3-CA1 regions of 0- to 1-day-old Sprague-Dawley rats. See Supplemental Experimental Procedures for details.

FM1-43 Staining, Destaining, and Quenching by BPB
Presynaptic boutons were stained with 7.5 μM FM1-43 (Molecular Probes) using field stimulation for 40 s at 30 Hz, followed by 60 s without stimulation to maximize the loading (Ryan et al., 1996). After 10 min washing with dye-free Tyrode's solution, individual boutons were destained by field stimulation. After a 120 s rest, multiple rounds of 90 mM K$^+$ solution were applied in the absence of FM dyes for 120 s with 120 s intervals. To define the TRP, at least three repetitive 90 mM K$^+$ applications were necessary because field stimulation was not enough to recycle all vesicles (Figure S4B). See Supplemental Experimental Procedures for details.

Transfection of Cultured Hippocampal Neurons with VAMP-EGFP Construct
See Supplemental Experimental Procedures.

Quenching of VAMP-EGFP by BPB
All transfected neurons were pretreated with 1 μM bafilomycin (Calbiochem, CA) in MEM without CNQX or D,L-AP5 for 1–3 hr at 37°C. They were transferred to Tyrode at room temperature and were kept in 1 μM bafilomycin throughout the experiment. In the standard protocol, plasma membrane fluorescence was first quenched by BPB, imaging was initiated, and vesicular fluorescence was quenched in the continued presence of BPB by stimulating vesicle turnover with field stimulation and multiple applications of 90 mM K$^+$ solution. VAMP-EGFP quenching by BPB was normalized to the TRP size according to the protocol in Figure S4A.

Optical Measurement and Analysis
See Supplemental Experimental Procedures.

Supplemental Data
The Supplemental Data include Supplemental Experimental Procedures and five supplemental figures and can be found with this article online at http://www.neuron.org/cgi/content/full/49/2/243/DC1/.

References

Aldrich, R.W., Corey, D.P., and Stevens, C.F. (1983). A reinterpretation of mammalian sodium channel gating based on single channel recording. Nature 306, 436–441.

Ales, E., Tabares, L., Poyato, J.M., Valero, V., Lindau, M., and Alvarez de Toledo, G. (1999). High calcium concentrations shift the mode of exocytosis to the kiss-and-run mechanism. Nat. Cell Biol. 1, 40–44.

An, S., and Zenisek, D. (2004). Regulation of exocytosis in neurons and neuroendocrine cells. Curr. Opin. Neurobiol. 14, 522–530.

Aravanis, A.M., Pyle, J.L., and Tsien, R.W. (2003a). Single synaptic vesicles fusing transiently and successively without loss of identity. Nature 423, 643–647.

Aravanis, A.M., Pyle, J.L., Harata, N.C., and Tsien, R.W. (2003b). Imaging single synaptic vesicles undergoing repeated fusion events: kissing, running, and kissing again. Neuropharmacology 45, 797–813.

Ceccarelli, B., Hurlbut, W.P., and Mauro, A. (1973). Turnover of transmitter and synaptic vesicles at the frog neuromuscular junction. J. Cell Biol. 57, 499–524.

Cochilla, A.J., Angleson, J.K., and Betz, W.J. (1999). Monitoring secretory membrane with FM1-43 fluorescence. Annu. Rev. Neurosci. 22, 1–10.

Dickman, D.K., Horne, J.A., Meinertzhagen, I.A., and Schwarz, T.L. (2005). A slowed classical pathway rather than kiss-and-run mediates endocytosis at synapses lacking synaptojanin and endophilin. Cell 123, 521–533.

Fernandez-Alfonso, T., and Ryan, T.A. (2004). The kinetics of synaptic vesicle pool depletion at CNS synaptic terminals. Neuron 41, 943–953.

Gandhi, S.P., and Stevens, C.F. (2003). Three modes of synaptic vesicular recycling revealed by single-vesicle imaging. Nature 423, 607–613.

Harata, N., Pyle, J.L., Aravanis, A.M., Mozhayeva, M., Kavalali, E.T., and Tsien, R.W. (2001). Limited numbers of recycling vesicles in small CNS nerve terminals: implications for neural signaling and vesicular cycling. Trends Neurosci. 24, 637–643.

Heuser, J.E. (1989). Review of electron microscopic evidence favouring vesicle exocytosis as the structural basis for quantal release during synaptic transmission. Q. J. Exp. Physiol. 74, 1051–1069.

Heuser, J.E., and Reese, T.S. (1973). Evidence for recycling of synaptic vesicle membrane during transmitter release at the frog neuromuscular junction. J. Cell Biol. 57, 315–344.

Hsu, S.F., Augustine, G.J., and Jackson, M.B. (1996). Adaptation of Ca^{2+}-triggered exocytosis in presynaptic terminals. Neuron 17, 501–512.

Jahn, R., Lang, T., and Sudhof, T.C. (2003). Membrane fusion. Cell 112, 519–533.

Kavalali, E.T., Klingauf, J., and Tsien, R.W. (1999). Properties of fast endocytosis at hippocampal synapses. Philos. Trans. R. Soc. Lond. B Biol. Sci. 354, 337–346.

Klingauf, J., Kavalali, E.T., and Tsien, R.W. (1998). Kinetics and regulation of fast endocytosis at hippocampal synapses. Nature 394, 581–585.

Klyachko, V.A., and Jackson, M.B. (2002). Capacitance steps and fusion pores of small and large-dense-core vesicles in nerve terminals. Nature 418, 89–92.

Koenig, J.H., and Ikeda, K. (1996). Synaptic vesicles have two distinct recycling pathways. J. Cell Biol. 135, 797–808.

Li, Z., and Murthy, V.N. (2001). Visualizing postendocytic traffic of synaptic vesicles at hippocampal synapses. Neuron *31*, 593–605.

Liu, G., and Tsien, R.W. (1995). Properties of synaptic transmission at single hippocampal synaptic boutons. Nature *375*, 404–408.

Miller, T.M., and Heuser, J.E. (1984). Endocytosis of synaptic vesicle membrane at the frog neuromuscular junction. J. Cell Biol. *98*, 685–698.

Murthy, V.N., and De Camilli, P. (2003). Cell biology of the presynaptic terminal. Annu. Rev. Neurosci. *26*, 701–728.

Palfrey, H.C., and Artalejo, C.R. (1998). Vesicle recycling revisited: rapid endocytosis may be the first step. Neuroscience *83*, 969–989.

Pyle, J.L., Kavalali, E.T., Piedras-Renteria, E.S., and Tsien, R.W. (2000). Rapid reuse of readily releasable pool vesicles at hippocampal synapses. Neuron *28*, 221–231.

Richards, D.A., Bai, J., and Chapman, E.R. (2005). Two modes of exocytosis at hippocampal synapses revealed by rate of FM1–43 efflux from individual vesicles. J. Cell Biol. *168*, 929–939.

Rizzoli, S.O., and Betz, W.J. (2005). Synaptic vesicle pools. Nat. Rev. Neurosci. *6*, 57–69.

Royle, S.J., and Lagnado, L. (2003). Endocytosis at the synaptic terminal. J. Physiol. *553*, 345–355.

Ryan, T.A. (2003). Kiss-and-run, fuse-pinch-and-linger, fuse-and-collapse: the life and times of a neurosecretory granule. Proc. Natl. Acad. Sci. USA *100*, 2171–2173.

Ryan, T.A., Reuter, H., Wendland, B., Schweizer, F.E., Tsien, R.W., and Smith, S.J. (1993). The kinetics of synaptic vesicle recycling measured at single presynaptic boutons. Neuron *11*, 713–724.

Ryan, T.A., Smith, S.J., and Reuter, H. (1996). The timing of synaptic vesicle endocytosis. Proc. Natl. Acad. Sci. USA *93*, 5567–5571.

Sankaranarayanan, S., and Ryan, T.A. (2000). Real-time measurements of vesicle-SNARE recycling in synapses of the central nervous system. Nat. Cell Biol. *2*, 197–204.

Sankaranarayanan, S., and Ryan, T.A. (2001). Calcium accelerates endocytosis of vSNAREs at hippocampal synapses. Nat. Neurosci. *4*, 129–136.

Sankaranarayanan, S., De Angelis, D., Rothman, J.E., and Ryan, T.A. (2000). The use of pHluorins for optical measurements of presynaptic activity. Biophys. J. *79*, 2199–2208.

Sara, Y., Mozhayeva, M.G., Liu, X., and Kavalali, E.T. (2002). Fast vesicle recycling supports neurotransmission during sustained stimulation at hippocampal synapses. J. Neurosci. *22*, 1608–1617.

Slepnev, V.I., and De Camilli, P. (2000). Accessory factors in clathrin-dependent synaptic vesicle endocytosis. Nat. Rev. Neurosci. *1*, 161–172.

Staal, R.G., Mosharov, E.V., and Sulzer, D. (2004). Dopamine neurons release transmitter via a flickering fusion pore. Nat. Neurosci. *7*, 341–346.

Stevens, C.F., and Williams, J.H. (2000). "Kiss and run" exocytosis at hippocampal synapses. Proc. Natl. Acad. Sci. USA *97*, 12828–12833.

Sudhof, T.C. (2004). The synaptic vesicle cycle. Annu. Rev. Neurosci. *27*, 509–547.

Taraska, J.W., Perrais, D., Ohara-Imaizumi, M., Nagamatsu, S., and Almers, W. (2003). Secretory granules are recaptured largely intact after stimulated exocytosis in cultured endocrine cells. Proc. Natl. Acad. Sci. USA *100*, 2070–2075.

Tsuboi, T., Zhao, C., Terakawa, S., and Rutter, G.A. (2000). Simultaneous evanescent wave imaging of insulin vesicle membrane and cargo during a single exocytotic event. Curr. Biol. *10*, 1307–1310.

Valtorta, F., Meldolesi, J., and Fesce, R. (2001). Synaptic vesicles: is kissing a matter of competence? Trends Cell Biol. *11*, 324–328.

Verstreken, P., Kjaerulff, O., Lloyd, T.E., Atkinson, R., Zhou, Y., Meinertzhagen, I.A., and Bellen, H.J. (2002). Endophilin mutations block clathrin-mediated endocytosis but not neurotransmitter release. Cell *109*, 101–112.

Wu, L.G. (2004). Kinetic regulation of vesicle endocytosis at synapses. Trends Neurosci. *27*, 548–554.

Xu, J., and Wu, L.-G. (2005). The decrease in the presynaptic calcium current is a major cause of short-term depression at a calyx-type synapse. Neuron *46*, 633–645.

Zenisek, D., Steyer, J.A., Feldman, M.E., and Almers, W. (2002). A membrane marker leaves synaptic vesicles in milliseconds after exocytosis in retinal bipolar cells. Neuron *35*, 1085–1097.

Zhou, Q., Petersen, C.C., and Nicoll, R.A. (2000). Effects of reduced vesicular filling on synaptic transmission in rat hippocampal neurones. J. Physiol. *525*, 195–206.